Identification of Potent and Novel α4β1 Antagonists Using in Silico Screening

Juswinder Singh,*,† Herman van Vlijmen,† Yusheng Liao,† Wen-Cherng Lee,† Mark Cornebise,† Mary Harris,† I-hsiang Shu,† Alan Gill,† Julio H. Cuervo,† William M. Abraham,§ and Steven P. Adams†

Department of Drug Design and Evaluation, Biogen Inc., 12 Cambridge Center, Cambridge, MA 02142, and Mount Sinai Medical Center, Miami Beach, FL 33140

Received February 5, 2002

The antigen α4β1 (very late antigen-4, VLA-4) plays an important role in the migration of white blood cells to sites of inflammation. It has been implicated in the pathology of a variety of diseases including asthma, multiple sclerosis, and rheumatoid arthritis. We describe a series of potent inhibitors of α4β1 that were discovered using computational screening for replacements of the peptide region of an existing tetrapeptide-based α4β1 inhibitor (**1**; 4-[*N*′-(2-methylphenyl)-ureido]phenylacetyl-Leu-Asp-Val) derived from fibronectin. The search query was constructed using a model of **1** that was based upon the X-ray conformation of the related integrin-binding region of vascular cell adhesion molecule-1 (VCAM-1). The 3D search query consisted of the N-terminal cap and the carboxyl side chain of **1** because, upon the basis of existing structure−activity data on this series, these were known to be critical for high-affinity binding to α4β1. The computational screen identified 12 reagents from a virtual library of 8624 molecules as satisfying the model and our synthetic filters. All of the synthesized compounds tested inhibit α4β1 association with VCAM-1, with the most potent compound having an IC_{50} of 1 nM, comparable to the starting compound. Using CATALYST, a 3D QSAR was generated that rationalizes the variation in activities of these α4β1 antagonists. The most potent compound was evaluated in a sheep model of asthma, and a 30 mg nebulized dose was able to inhibit early and late airway responses in allergic sheep following antigen challenge and prevented the development of nonspecific airway hyperresponsiveness to carbachol. Our results demonstrate that it is possible to rapidly identify nonpeptidic replacements of integrin peptide antagonists. This approach should be useful in identification of nonpeptidic α4β1 inhibitors with improved pharmacokinetic properties relative to their peptidic counterparts.

Introduction

The antigen α4β1 (VLA-4, very late antigen-4) is a member of the integrin family and is involved in the migration of mononuclear leukocytes to sites of inflammation. Due to the role of α4β1 in the inflammatory response, it is an attractive target for therapeutic intervention. The α4-integrin-dependent adhesion pathways are critical intervention points in several inflammatory and autoimmune pathologies. These include asthma,[1] multiple sclerosis,[2,3] and rheumatoid arthritis.[4]

The antigen α4β1 is known to bind fibronectin in the extracellular matrix and vascular cell adhesion molecule-1 (VCAM-1) on the endothelium. Komoriya et al.,[5] using peptide mapping studies, were able to identify the minimum fibronectin sequence for cell adhesion activity as being Leu-Asp-Val. This integrin-binding motif was used as the starting point in the design of small molecule antagonists of α4β1. Lin et al.[6] used a novel capping strategy to identify 4-[*N*′-(2-methylphenyl)ureido]phenylacetyl-Leu-Asp-Val (**1**) as a potent, highly selective inhibitor of α4β1. This class of compounds exhibits efficacy in inflammatory models such as the sheep model of allergic bronchoconstriction;[6] however, their peptidic nature results in rapid clearance in animals (S.P.A., unpublished results). It would therefore be useful to identify alternative nonpeptidic structures to replace the Leu-Asp-Val portion of the inhibitors to yield compounds with better pharmacokinetic properties while maintaining potency.

Database mining has emerged as a productive way to identify more favorable replacements for peptide fragments in lead molecules. One approach involves defining a three-dimensional pharmacophore model for the ligand and searching a chemical database of existing compounds for those structures that satisfy the spatial and chemical constraints of the model.[7] Computational tools such as CATALYST[8] and UNITY3D[9] have been utilized successfully to identify novel inhibitors of HIV-integrase[10], as well as the angiotensin II[11] and the muscarinic M3 receptor.[12] In this paper, the application of this approach to the discovery of novel nonpeptidic VLA-4 antagonists is described.

Results

Model Building and Database Searching. To discover novel replacements of the Leu-Asp-Val portion of our peptidic inhibitors, **1** was used as a template to build a 3D query, which consisted of the PUPA (4-[N′-(2-methylphenyl)ureido]phenylacetyl) and the carboxyl group (Figure 1). These groups were selected upon the basis of structure−activity data that showed that they were critical for high-affinity binding. For example, we have shown previously that the starting peptide has weak binding to α4β1 (Ile-Leu-Asp-Val ≈ 66 μM)[6]

* To whom correspondence should be addressed. Phone: (617)679-2027. Fax: (617)679-2616. E-mail: Juswinder_Singh@biogen.com.
† Biogen Inc.
§ Mount Sinai Medical Center.

10.1021/jm020054e CCC: $22.00
Published on Web 06/11/2002

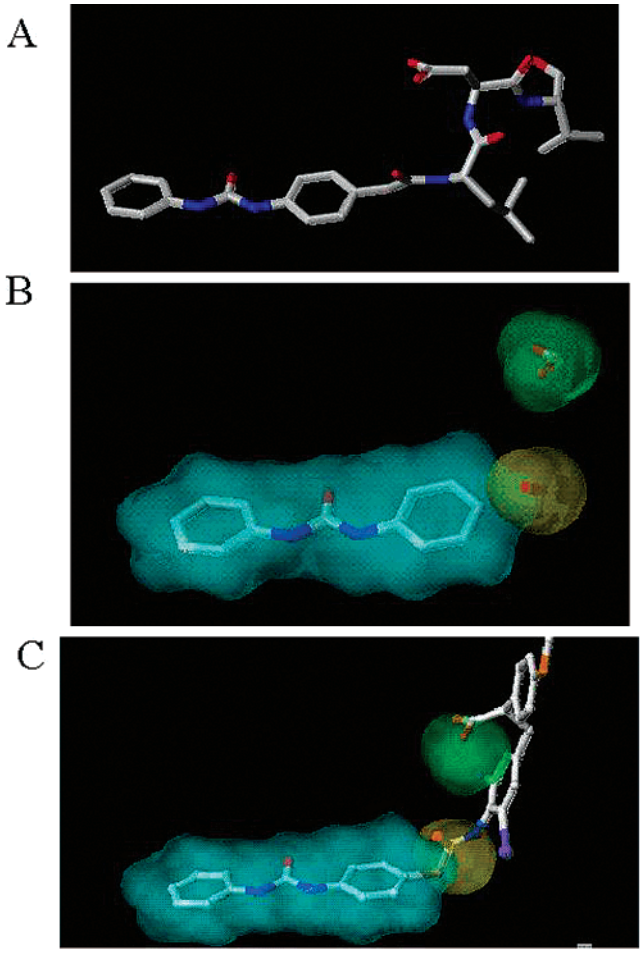

Figure 1. In silico screening for Leu-Asp-Val replacements: (a) the 3-D conformation of **1** used to build the 3D CATALYST search query; (b) the CATALYST search query (hypothesis) consisting of PUPA (cyan and yellow) and carboxyl group (green) from **1**; (c) overlay of a compound from the in silico screen with the search query.

and that addition of the N-terminal cap PUPA results in a 100 000-fold enhancement in binding affinity. The PUPA alone does not inhibit the integrin. The aspartic acid side chain appears to be crucial for inhibition because deletion of the Asp-Val side chains to form PUPA-Leu results in complete loss of binding while truncation of Val, providing PUPA-Leu-Asp, results in only a 30-fold decrease in the inhibition of α4β1.[6]

The conformation of **1** was based on the X-ray crystal structure of the integrin binding region of VCAM-1, Ile-Asp-Ser, which is homologous to the Leu-Asp-Val portion of fibronectin and is known to bind to α4β1. The conformation of the N-terminal cap (PUPA) was determined from a systematic conformational energy search. The resulting 3D query was used to search a database of virtual compounds that consisted of commercially available reagents coupled to the N-terminal cap, PUPA. A search of the Available Chemicals Directory[13] for all compounds with a free amine or nitro group and a carboxyl group identified 8624 reagents. A virtual chemical library was created by coupling in silico the carboxyl of the N-terminal cap (PUPA) to the free amine or nitro of the commercially available reagent (Scheme 1). A multiconformational database of these virtual compounds was built and screened using our 3D query, resulting in 416 hits. At this stage, we removed peptide sequences, which accounted for a large fraction of the hits, leaving 170 compounds for consideration (2% of the initial database of 8624 reagents). From this set of approximately 170 reagents, 12 were selected on the basis of synthetic feasibility and commercial availability. A straightforward, three-step process of reduction, coupling to PUPA, and cleavage of the ester (Scheme 1) was used to produce the set of 12 compounds submitted to the in vitro assay (0.14% of the initial database of 8624 reagents).

Biological Results. A direct binding assay was used to evaluate the ability of the synthesized compounds to inhibit the interaction between VLA-4 and a VCAM−Ig fusion protein. All of the compounds synthesized from the commercially available templates derived from computational screening demonstrated inhibition in our direct binding assay, with the most potent compound (**2**, 1.3 nM) comparable in potency to the starting compound upon which the computational search query was based (**1**, 0.6 nM). The twelve compounds built from computational screening showed a wide range in inhibitory activity from 1.3 to 20 000 nM (Figure 2). The compound **2** was derived from a phenylpropionic acid template with a β-methyl substitution. The α-amide substituent of the phenylpropionic acid template also showed potent inhibition (**3**, 58 nM), although decreased relative to the β-methyl substituent. Interestingly, para substitution of the phenyl ring in the phenylpropionic template provided significantly more potent inhibition than meta substitution as reflected in the 2000-fold difference in activity exemplified by analogues **2** and **9**. Another potent template involved a urea group (**4**) with an IC_{50} of 67 nM. The remaining compounds were much less active (**5**−**13**, 800−20 000 nM).

In the sheep model of allergic airways disease, a single 30 mg dose of compound **2** administered 30 min before antigen challenge inhibited the immediate antigen-induced bronchial response by 48%. Late-phase bronchoconstriction and the antigen-induced nonspecific airway hyperresponsiveness to inhaled carbachol were almost completely eliminated (Figure 3).

To explain the structural basis for the variation in the activities of the compounds, a 3D QSAR model was built using CATALYST. The CATALYST program provides a feature-based description of chemical structures (e.g., H-bond acceptors, negative ionizable groups, etc.) and attempts to correlate the 3D arrangement of features across a compound set with their biological activities. The model that best accounted for the activities of the compounds consisted of a hydrogen-bond acceptor, a hydrogen-bond donor, a hydrophobic feature, and a custom-built *superfeature*, which described the PUPA. The model is shown in Figure 4, overlayed with the most potent compound, **2** ($IC_{50} \approx 1.3$ nM). All of the features are mapped by **2**, with the carboxyl satisfying the hydrogen-bond acceptor site and the β-methyl satisfying the hydrophobic site. The amide NH of **2** maps to the hydrogen-bond donor site, while the PUPA maps to our superfeature. The weaker potencies of **3** (IC_{50} = 58 nM) and **4** (IC_{50} = 67 nM**)** are attributed to inadequate mapping of the methyl site, although the other features are mapped well. It appears that the compounds **5**−**10** (IC_{50} = 800−3000 nM) fail to optimally

Scheme 1[a]

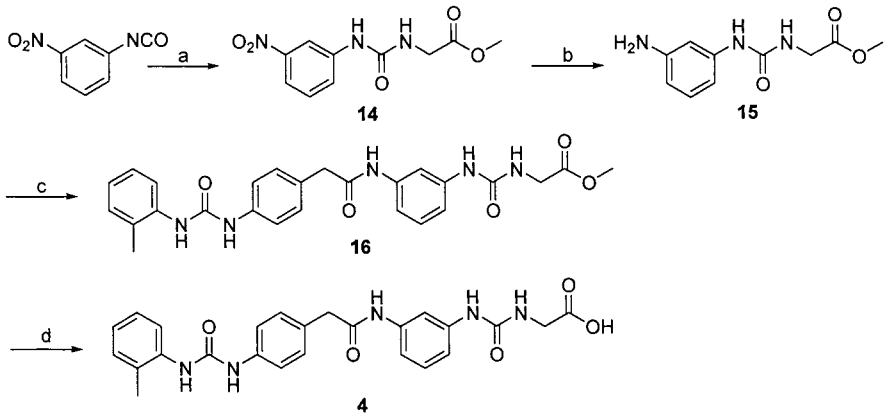

[a] Synthesis of **4**. Key: (a) glycine methyl ester hydrochloride, Et_3N, DMF; (b) H_2, Pd/C, MeOH; (c) 2-methyl-PUPA, HATU, DIEA, DMF; (d) LiOH, DMF.

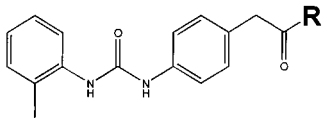

#	R	IC50 (μM)	#	R	IC50 (μM)
1	—Leu-Asp-Val-OH	0.0006			
2		*0.0013*	8	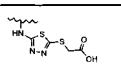	2.3
3		*0.058*	9	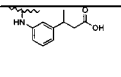	2.5
4	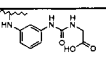	*0.067*	10	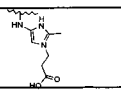	3
5	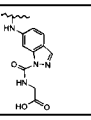	*0.8*	11	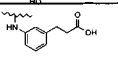	11.4
6	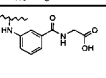	*1.2*	12	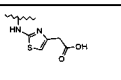	15
7	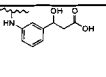	*2*	13	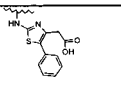	20

Figure 2. Structures and binding assay data for the compounds of this study derived from the database searching method.

map the superfeature site but are able to map all of the other features. Similarly, **11** (IC_{50} = 11 400 nM), **12** (IC_{50} = 16 000 nM), and **13** (IC_{50} = 20 000 nM) are unable to map the superfeature and have a poorer fit to the other features.

Conclusion

The successful transformation of a peptide lead compound to a nonpeptide epitope remains a significant challenge in drug discovery. We have demonstrated how in silico screening resulted in identifying novel potent nanomolar replacements for the peptidic portion of an existing α4β1 antagonist. We are now testing how useful

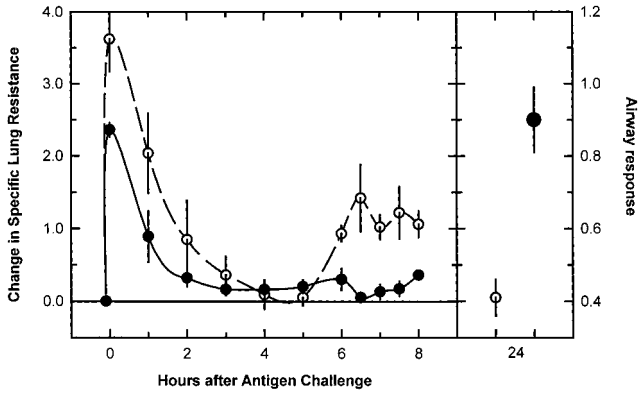

Figure 3. Effect of compound **2** on sheep airway responses to antigen. Naturally allergic sheep that were previously shown to exhibit both early and late bronchoconstrictor responses to nebulized *A. suum* antigens were used in the study. A 30 mg dose (~1 mg/kg) of **2** formulated as the Tris salt in saline was administered by an air-jet nebulizer 0.5 h prior to challenge with nebulized antigen. Specific lung resistance (SR_L) was determined periodically for drug-treated animals (●) over 8 h and is expressed as the change from prechallenge SR_L. Historical control resistance data following antigen challenge (○) is presented for the same animals that received drug in this study. Airway responsiveness was determined 24 h after antigen challenge by determining the cumulative dose of carbachol required to induce a 4-fold increase in SR_L. Results are expressed as the ratio of the carbachol dose in the presence or absence of drug treatment divided by the carbachol dose to induce the same increase before antigen challenge (right panel). The data are plotted as the mean ± SEM (mean ± 0.5(range)) for two sheep.

the pharmacophore model will be in improving the potencies of the micromolar inhibitors identified from the virtual screening. The efficacy of **2** to inhibit early and late airway responses in allergic sheep via aerosol administration is encouraging. We are presently attempting to improve the pharmacokinetics of this series, which will enable us to better assess the therapeutic utility of intervention at α4β1 in a broader range of animal models.

Experimental Section

Model Building. A 3D model of **1** was built using the BUILDER module within InsightII.[8] All energy calculations were performed using the CVFF force field within DISCOVER, and the potentials were set using the ForceField/Potential command.

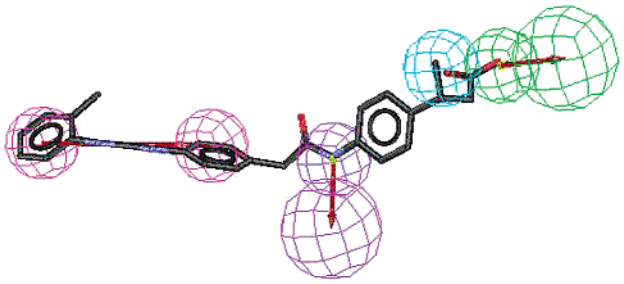

Figure 4. The alignment of **2** to the CATALYST model. The wireframe spheres represent CATALYST features: hydrogen-bond acceptor (green); hydrophobe (cyan); hydrogen-bond donor (purple); superfeature (pink).

The Leu-Asp-Val section of **1** was built using the side chain and main chain torsion angles from the Ile39-Asp40-Ser41 region from VCAM-1 (protein databank code 1VCA).[14] The N-terminal cap, termed PUPA, was attached onto the Leu-Asp-Val fragment. The N-terminal cap was energy minimized using 1000 steps of steepest descent, while the rest of the structure was held fixed. By use of a systematic conformational search, the lowest energy conformation of the N-terminal cap was identified. The systematic conformational search was carried out using the SEARCH/COMPARE module of INSIGHTII using the default settings with a 30° step size and the ENERGY option set to on. During the minimization, all atoms derived from the Ile39-Asp40-Ser41 region of VCAM-1 were held fixed. After each step in the conformational search the N-terminal cap was subjected to 500 steps of energy minimization using the Optimize option with the default parameters, and the lowest energy conformation was selected.

3D Query and Database Searching. The Available Chemical Directory[13] was screened for all compounds with a carboxyl group and either a free amine or nitro group. These commercially available reagents were computationally coupled to the free carboxyl group of our N-terminal cap (PUPA) via the free amine or nitro group using LEGION.[9]

With the use of CATALYST,[8] a multiconformer 3D database of the virtual library was created. For the conformer generation, the Fast conformer process was used with the MAXCONFS option set to 250 and the energy threshold set to 15 kcal/mol.

The 3D query that was used for database mining was based upon **1** and was built using CATALYST. The query was built using ViewHypothesis workbench and consisted of the PUPA and the carboxyl of **1**. A tolerance of 2.0 Å was used at each of the atomic positions.

CATALYST was also used to build a 3D QSAR of the compounds synthesized from the results of our database search. The IC_{50}'s used for the model generation were taken from Figure 2. The models were built using CATHYPO in CATALYST. The conformational models were built using the CATCONF module with the Best option set to on and the maximum number of conformations set to 250, and the energy threshold was set to 15 kcal/mol. All other parameters used were at their default settings. In addition to using the standard feature set supplied by CATALYST (hydrogen-bond donor, hydrogen-bond acceptor, negative ionizable, hydrophobe), a custom-built feature that described the PUPA portion of the compounds was added. Because all of the compounds had this feature, it was defined as a *superfeature* using the Exclude/Edit tool. This was necessary because the number of features presented by the compounds was much greater (as judged by the CONFIG value) than CATALYST could adequately sample. The superfeature consisted of two individual features describing the centroid of each of the phenyl rings of the PUPA connected by a vector. The best model had a correlation coefficient of 0.97 between the predicted and actual activities.

Biological Assay. The compounds were tested in binding assays, which have been reported in detail elsewhere.[15]

α4β1 Inhibitor Effects on Sheep Airway Responses to Antigen. Methods for assessing drug effects on antigen-induced increases in specific lung resistance (SR_L) are described elsewhere.[1] A 30 mg dose of **1** formulated in 5 mL of saline containing 2 mol equiv of Tris (pH 7.0−7.4) was administered by an air-jet nebulizer (Raindrop, Puritan, Bennett, Lenexa, KS) 0.5 h prior to challenge with nebulized *Ascaris suum* antigen. SR_L was determined periodically for drug-treated animals over 8 h. The change in SR_L was calculated for each sheep as the difference from prechallenge baseline SR_L, and values reported are the mean ± SEM (mean ± 0.5(range)) for two sheep. Airway responsiveness was determined 24 h after antigen challenge and is expressed as the cumulative dose of carbachol at 24 h required to induce a 4-fold increase in SR_L in the presence or absence of drug treatment divided by the carbachol dose to induce the same increase before antigen challenge. The protocol used in the sheep study was approved by the Mount Sinai Medical Center Animal Research Committee, which is responsible for ensuring the humane care and use of experimental animals.

Chemistry: General. Unless noted otherwise, all starting materials and synthesis reagents were obtained commercially and used without further purification. Abbreviations are as follows: DIEA, *N,N*-diisopropylethylamine; DMF, dimethylformamide; Et_3N, triethylamine; HATU, *O*-(7-azabenzotriazol-1-yl)-1,1,3,3-tetramethyluronium hexafluorophosphate; EDC, 1-ethyl-3-(3-dimethylaminopropyl)carbodiimide hydrochloride; 2-methylPUPA, 2-(4-(3-(*o*-methylphenyl)ureido)phenyl)acetic acid; TFA, trifluoroacetic acid.

Nuclear magnetic resonance spectra (NMR) were recorded as solutions in the indicated solvent on Bruker DPX-400 and AC-300. Chemical shifts are reported in parts per million (δ, ppm) using $CHCl_3$ or DMSO as an internal standard. Coupling constants are reported in hertz (Hz). Spectral splitting patterns are designated as follows: s, singlet; d, doublet; t, triplet; q, quartet; m, multiplet; br, broad.

Mass spectra were obtained on a Fisons VG Platform Quattro II mass spectrometer system and processed with MassLynx software. High-resolution mass spectra were performed by M-Scan Inc. (West Chester, PA) on a VG Analytical ZAB 2SE high-field mass spectrometer.

Analytical HPLC was performed on a Perkin-Elmer 200 Series HPLC system with UV detection at 214 or 254 nm or both on an Applied Biosystems 785A programmable absorption detector. Data analysis was run using a PE Nelson 1020 integrator. A Higgins Analytical C-18 reverse-phase column (3 μm pore size, 4.6 mm × 15 cm) was utilized and was running with a 7 min gradient using H_2O (containing 0.1% TFA v/v) and CH_3CN (containing 0.085% TFA v/v) as the mobile phase. Preparative HPLC was performed with a Rainin HPLX solvent delivery system with a Rainin Dynamax UV-1 detector (set at 225 nm) using a Rainin Microsorb C-18 reverse-phase column (5 μm pore size, 21.4 mm × 25 cm) eluted at 12 mL/min using the same solvent system as for the analytical HPLC. Fractions were collected and checked for purity with analytical HPLC, and pure fractions were combined and evaporated in vacuo to provide purified material.

All new compounds show analytical and spectral (^{1}H NMR, MS) data consistent with the depicted structures. All reactions were conducted at room temperature unless otherwise noted, and were followed to completion by analytical HPLC.

Synthesis of compound 4 (see Scheme 1): Methyl 2-(3-(3-nitrophenyl)ureido)acetate (4). To a solution of glycine methyl ester hydrochloride (0.842 g, 6.7 mmol) in DMF (10 mL) was added Et_3N (2.8 mL, 20 mmol) with stirring to give a colorless solution. To this was added 3-nitrophenylisocyanate (1.0 g, 6.1 mmol) in portions over 5 min to give a yellow solution. After stirring 14 h, the solution was diluted with ethyl acetate (EtOAc), washed three times with 1 N HCl and then with brine, dried ($MgSO_4$), and concentrated in vacuo to a thick yellow oil. The product was recrystallized twice from EtOAc/hexanes and then again from ethanol/water to give 1.0 g (65%) of compound **14** as fine, pale-yellow needles (HPLC, >99%). MS: *m/z* 254 $(M + H)^+$.

General Procedure b for Reduction of a Nitro Group to the Corresponding Amine. Methyl 2-(3-(3-aminophenyl)ureido)acetate (15). To solution of **14** (0.5 g, 1.98 mmol) in 15 mL of methanol (MeOH) in a 90 mL Pyrex high-pressure vessel flushed with nitrogen was added 10% palladium on carbon (ca. 100 mg). The vessel was capped with a hydrogenation head, flushed with nitrogen, and then charged with hydrogen (60 psi), and the mixture was allowed to stir for 14 h. The system was purged with nitrogen, and the mixture was filtered through a plug of Celite 545. The Celite plug was washed with additional MeOH, and the combined filtrate was concentrated in vacuo to give 0.44 g (99%) of compound **15** as a foamy white solid that was used without further purification. MS: *m/z* 224 $(M + H)^+$.

General Procedure c for Coupling 2-Methyl-PUPA to Amine. Methyl 2-(3-(3-(2-Methyl)PUPacetamidophenyl)-ureido)acetate (16). To a mixture of **15** (0.23 g, 1.03 mmol), 2-methyl-PUPA[1] (0.284 g, 1.0 mmol), and HATU (0.456 g, 1.2 mmol) in 6 mL of DMF was added DIEA (0.7 mL, 4 mmol) to give a dark yellow solution. The mixture was stirred for 2 h and then diluted with EtOAc, washed three times with 1 N HCl and then brine, dried ($MgSO_4$), and concentrated in vacuo to give a yellow solid. Three iterations of dissolution/precipitation from acetone/hexane gave 0.352 g (72%) of compound **16** as an off-white solid (HPLC, >98%). MS: *m/z* 490 $(M + H)^+$. (EDC and Et_3N were used as the coupling reagents for compounds **2**, **3**, **12**, **13**.)

General procedure d for Hydrolysis of Esters. 2-(3-(3-(2-Methyl)PUPacetamidophenyl)ureido)acetic acid (4). To a solution of **16** (0.1 g, 0.2 mmol) in 4 mL of DMF was added aqueous 2 N LiOH (0.5 mL, 1.0 mmol). The resulting solution was stirred for 2 h and then slowly poured into 150 mL of aqueous 1 N HCl to give a white precipitate. The solid material was filtered off, washed with H_2O, and dried in vacuo to give 90 mg (95%) of compound **4** as a fine, beige solid (HPLC, >99%). MS: *m/z* 476 $(M + H)^+$.

Compounds **2**, **4**, **5**, **6**, **7**, **8**, **9**, **10**, and **11** were synthesized using the general procedures b, c, and d. Compounds **3**, **12**, and **13** were synthesized using the general procedures c and d. Analytical samples were obtained from preparative HPLC purification except compound **4** which was obtained by precipitation as described in the procedure.

Spectral Data. Compound 2: ^{1}H NMR (400 MHz, DMSO-d_6) δ 9.98 (s, 1 H), 8.92 (s, 1 H), 7.82 (s, 1 H), 7.75 (d, J = 7.9 Hz, 2 H), 7.41 (d, J = 8.5 Hz, 2 H), 7.32 (d, J = 8.5 Hz, 2 H), 7.15 (d, J = 8.5 Hz, 1 H), 7.05 (m, 4 H), 6.85 (m, 1 H), 3.46 (s, 2 H), 3.00 (m, 1 H), 2.37 (d, J = 7.5 Hz, 2 H), 2.15 (s, 3 H), 1.09 (d, J = 6.9 Hz, 3 H); ^{13}C NMR (100 MHz, DMSO-d_6) δ 173.5, 169.5, 153.0, 141.2, 138.7, 137.8, 137.7, 130.5, 129.7, 129.6, 127.7, 127.2, 126.5, 122.9, 121.3, 119.5, 118.4, 43.0, 42.6, 35.7, 22.4, 18.2; FABMS, *m/z* 446 $(M + H)^+$; HRMS *m/z* $(M + H)^+$ calcd 446.2080, obsd 446.2082.

Compound 3: ^{1}H NMR (400 MHz, DMSO-d_6) δ 10.02 (s, 1 H), 9.01 (s, 1 H), 8.06 (d, J = 8.1 Hz, 1 H), 7.91 (s, 1 H), 7.76 (d, J = 7.8 Hz, 1 H), 7.42 (d, J = 8.5 Hz, 2 H), 7.34 (d, J = 8.5 Hz, 1 H), 7.27 (d, J = 8.5 Hz, 2 H), 7.08 (m, 4 H), 6.86 (m, 1 H), 4.28 (m, 1 H), 3.48 (s, 2 H), 2.90 (m, 1 H), 2.2.70 (m, 1 H), 2.16 (s, 3 H), 1.70 (s, 3 H); ^{13}C NMR (100 MHz, DMSO-d_6) δ 173.5, 169.6, 169.5, 153.0, 138.8, 138.0, 137.8, 132.8, 130.5, 129.8, 129.6 (two peaks), 127.8, 126.5, 122.9, 121.4, 119.3, 118.4, 54.0, 43.0, 36.6, 22.7, 18.2; FABMS, *m/z* 489 $(M + H)^+$; HRMS *m/z* $(M + H)^+$ calcd 489.2138, obsd 489.2122.

Compound 4: ^{1}H NMR (400 MHz, DMSO-d_6) δ 10.04 (s, 1 H), 8.97 (s, 1 H), 8.76 (s, 1 H), 7.87 (s, 1 H), 7.83 (d, J = 8.0 Hz, 1 H), 7.70 (s, 1 H), 7.39 (d, J = 8.4 Hz, 2 H), 7.22 (d, J = 8.4 Hz, 2 H), 7.20−7.10 (m, 5 H), 6.92 (t, J = 7.2 Hz, 1 H), 6.30 (br s, 1 H), 3.78 (br d, 2 H), 3.54 (s, 2 H), 2.22 (s, 3 H); ^{13}C NMR (100 MHz, DMSO-d_6) δ 172.5, 169.7, 155.4, 153.0, 140.9, 139.9, 138.7, 137.8, 130.5, 129.7, 129.2, 127.8, 126.5, 122.9, 121.3, 118.4, 113.0, 112.6, 109.0, 43.1, 41.6, 18.2; MS (EI) *m/z* 476 $(M + H)^+$; HRMS *m/z* $(M + H)^+$ calcd 476.1934, obsd 476.1959.

Compound 5: ^{1}H NMR (400 MHz, DMSO-d_6) δ 10.43 (s, 1 H), 8.98 (s, 1 H), 8.68 (s, 1 H), 8.30 (s, 1 H), 7.87 (s, 1 H), 7.83 (d, J = 7.6 Hz, 1 H), 7.77 (d, J = 8.7 Hz, 1 H), 7.53 (dd, J = 8.8, 1.8 Hz, 1 H), 7.40 (d, J = 8.5 Hz, 2 H), 7.25 (d, J = 8.5 Hz, 2 H), 7.14 (m, 2 H), 6.92 (t, J = 7.4 Hz, 1 H), 3.93 (br s, 2 H), 3.61 (s, 2 H), 2.22 (s, 3 H); MS (EI) *m/z* 501 $(M + H)^+$; HRMS *m/z* $(M + H)^+$ calcd 501.1886, obsd 501.1921.

Compound 6: ^{1}H NMR (400 MHz, DMSO-d_6) δ 10.28 (s, 1 H), 8.97 (s, 1 H), 8.74 (t, J = 5.9 Hz, 1 H), 8.05 (s, 1 H), 7.87 (s, 1 H), 7.83 (d, J = 7.6 Hz, 1 H), 7.79 (br d, J = 8.0 Hz, 1 H), 7.51 (d, J = 7.8 Hz, 1 H), 7.39 (m, 3 H), 7.24 (d, J = 8.5 Hz, 2 H), 7.16−7.10 (m, 2 H), 6.92 (t, J = 7.4 Hz, 1 H), 3.89 (d, J = 5.9 Hz, 2 H), 3.57 (s, 2 H), 2.22 (s, 3 H); MS (EI) *m/z* 461 $(M + H)^+$; HRMS *m/z* $(M + H)^+$ calcd 461.1825, obsd 461.1854.

Compound 7: ^{1}H NMR (400 MHz, DMSO-d_6) δ 10.09 (s, 1 H), 8.96 (s, 1 H), 7.87 (s, 1 H), 7.83 (d, J = 7.9 Hz, 1 H), 7.57 (s, 1 H), 7.51 (d, J = 8.1 Hz, 1 H), 7.39 (d, J = 8.5 Hz, 2 H), 7.22 (m, 3 H), 7.14 (m, 2 H), 6.99 (d, J = 7.7 Hz, 1 H), 6.92 (t, J = 7.4 Hz, 1 H), 4.87 (t, J = 6.8 Hz, 1 H), 3.55 (s, 2 H), 2.47 (d, J = 6.5 Hz, 2 H), 2.22 (s, 3 H); MS (EI) *m/z* 448 $(M + H)^+$; HRMS *m/z* $(M + H)^+$ calcd 448.1872, obsd 448.1857.

Compound 8: ^{1}H NMR (400 MHz, DMSO-d_6) δ 10.06 (s, 1 H), 8.96 (s, 1 H), 7.87 (s, 1 H), 7.82 (d, J = 7.5 Hz, 1 H), 7.44 (m, 2 H), 7.39 (d, J = 8.5 Hz, 2 H), 7.23 (d, J = 8.5 Hz, 2 H), 7.14 (m, 3 H), 6.92 (t, J = 7.4 Hz, 2 H), 3.54 (s, 2 H), 3.07 (m, 1 H), 2.45 (d, J = 7.4 Hz, 2 H), 2.22 (s, 3 H). MS (EI) *m/z* 446 $(M + H)^+$; HRMS *m/z* $(M + H)^+$ calcd 446.2080, obsd 446.2082.

Compound 9: ^{1}H NMR (400 MHz, DMSO-d_6) δ 10.30 (s, 1 H), 8.95 (s, 1 H), 7.86 (s, 1 H), 7.83 (d, J = 7.6 Hz, 1 H), 7.36 (d, J = 8.5 Hz, 2 H), 7.19 (d, J = 8.5 Hz, 2 H), 7.14 (m, 2 H), 7.05 (s, 1 H), 6.92 (t, J = 7.5 Hz, 1 H), 4.00 (t, J = 6.7, 2 H), 3.47 (s, 2 H), 2.63 (t, J = 6.7, 2 H), 2.24 (s, 3 H), 2.22 (s, 3 H); MS (EI) *m/z* 435 $(M + H)^+$; HRMS *m/z* $(M + H)^+$ calcd 436.1985, obsd 436.1980.

Compound 10: ^{1}H NMR (400 MHz, DMSO-d_6) δ 10.07 (s, 1 H), 9.14 (s, 1 H), 7.98 (s, 1 H), 7.83 (d, J = 7.5 Hz, 1 H), 7.41 (m, 4 H), 7.22 (d, J = 8.5 Hz, 2 H), 7.15 (m, 4 H), 6.90 (t, J = 7.5 Hz, 2 H), 3.54 (s, 2 H), 2.76 (t, J = 7.5 Hz, 2 H), 2.48 (d, J = 7.5 Hz, 2 H), 2.23 (s, 3 H); MS (EI) *m/z* 432 $(M + H)^+$; HRMS *m/z* $(M + H)^+$ calcd 432.1923, obsd 432.1911.

Compound 11: ^{1}H NMR (400 MHz, DMSO-d_6) δ 10.30 (s, 1 H), 9.01 (s, 1 H), 7.90 (s, 1 H), 7.82 (d, J = 7.8 Hz, 1 H), 7.40 (d, J = 8.5 Hz, 2 H), 7.21 (d, J = 8.5 Hz, 2 H), 7.14 (m, 2 H), 6.92 (m, 1 H), 4.04 (s, 2 H), 3.73 (s, 2 H), 2.22 (s, 3 H); MS (EI) *m/z* 458 $(M + H)^+$; HRMS *m/z* $(M + H)^+$ calcd 458.0957, obsd 458.0970.

Compound 12: ^{1}H NMR (400 MHz, DMSO-d_6) δ 8.95 (s, 1 H), 7.84 (s, 1 H), 7.77 (d, J = 7.3 Hz, 1 H), 7.34 (d, J = 8.6 Hz, 2 H), 7.16 (d, J = 8.6 Hz, 2 H), 7.06 (m, 2 H), 6.86 (m, 2 H), 3.59 (s, 2 H), 3.52 (s, 2 H), 2.47 (s, 1 H), 2.16 (s, 3 H, Me); ^{13}C NMR (75 MHz, DMSO-d_6) δ 171.9, 169.7, 157.8, 153.0, 144.6, 139.0, 137.8, 130.5, 129.9, 128.4, 127.7, 126.4, 121.3, 118.4, 110.4, 41.4, 37.2, 18.2; FABMS, *m/z* 425 $(M + H)^+$; HRMS *m/z* $(M + H)^+$ calcd 425.1284, obsd 425.1293.

Compound 13: ^{1}H NMR (400 MHz, DMSO-d_6) δ 8.94 (s, 1 H), 7.83 (s, 1 H), 7.51 (m, 2 H), 7.41−7.29 (m, 5 H), 7.18 (d, J = 8.5 Hz, 2 H), 7.10 (d, J = 87.9 Hz, 1 H), 7.05 (d, J = 7.7 Hz, 1 H), 6.87 (m, 1 H), 6.45 (m, 1 H), 3.75 (s, 2 H), 3.63 (s, 2 H), 2.17 (s, 3 H, Me); FABMS, *m/z* 501 $(M + H)^+$; HRMS *m/z* $(M + H)^+$ calcd 501.1597, obsd 501.1581.

Acknowledgment. We thank Diane Leone, William Yang, and Dan Scott for generating the in vitro biological data. Also, we thank Paul Lyne, Parul Matani, Prashant Singh, Laurie Castonguay and Russ Petter for critical evaluation of the manuscript.

References

(1) Abraham, W. M.; Sielczak, M. W.; Ahmed, A.; Cortes, A.; Lauredo, I. T.; Kim, J.; Pepinsky, B.; Benjamin, C. D.; Leone, D. R.; Lobb, R. R.; Weller, P. F. a4-Integrins Mediate Antigen-induced Late Bronchial Responses and Prolonged Airway Hyperresponsiveness in Sheep. *J. Clin. Invest.* **1994**, *93*, 776−787.

(2) Chabot, S.; Williams, G.; Yong, V. W. Microglial production of TNF-alpha is induced by activated T lymphocytes. Involvement of VLA-4 and inhibition by interferonbeta-1β. *J. Clin. Invest.* **1997**, *100*, 604−612.
(3) Leger, O. J.; Yednock, T. A.; Tanner, L.; Horner, H. C.; Hines, D. K.; Keen, S.; Saldanha, J. Humanization of a mouse antibody against human alpha-4 integrin: a potential therapeutic for the treatment of multiple sclerosis. *Hum. Antibodies* **1997**, *8*, 3−16.
(4) Seiffge, D. Protective effects of monoclonal antibody to VLA-4 on leukocyte adhesion and course of disease in adjuvant arthritis in rats. *J. Rheumatol.* **1996**, *23*, 2086−91.
(5) Komoriya, A.; Green, L. J.; Mervic, M.; Yamada, S. S.; Yamada, K. M.; Humphries, M. J. The minimal essential sequence for a major cell type-specific adhesion site(CS1) within the alternatively spliced Type III connecting segment domain of fibronectin is Leucine-Aspartic Acid-Valine. *J. Biol. Chem.* **1991**, *266*, 15075−15079.
(6) Lin, K. C.; Ateeq, H. S.; Hsiung, H. S.; Chong, L. T.; Zimmerman, C. N.; Castro, A.; Lee, W.-c.; Hammond, C. E.; Kalkunte, S.; Chen, L.-L.; Pepinsky, R. B.; Leone, D. R.; Sprague, A. G.; Abraham, W. M.; Gill, A.; Lobb, R. R.; Adams, S. P. Selective, Tight-Binding Inhibitors of Integrin α4β1 That Inhibit Allergic Airway Responses. *J. Med. Chem.* **1999**, *42*, 920−934.
(7) Milne, G.; Nicklaus, M.; Wang, S. S Pharmacophores in drug Design and Discovery. *QSAR Environ. Res.* **1998**, *9*, 23−38.
(8) *InsightII*; Accelrys: San Diego, CA, 1998.
(9) *Legion*; Tripos: St. Louis, MO, 1998.
(10) Nicklaus, M. C.; Neamati, N.; Hong, H.; Mazumder, A.; Sunder, S.; Chen, J.; Milne, G. W. A.; Pommier, Y. HIV-1 Integrase Pharmacophore: Discovery of Inhibitors through 3-Dimensional Database Searching. *J. Med. Chem.* **1997**, *40*, 920−929.
(11) Kiyama, R.; Honma, T.; Hayashi, K.; Ogawa, M.; Hara, M.; Fujimoto, M.; Fujishita, T. Novel Angiotensin II Receptor Antagonists. Design, Synthesis, and in Vitro Evaluation of Dibenzo[a,d]cycloheptene and Dibenzo[b,f]oxepin Derivatives. Searching for Bioisosteres of Biphenylyltetrazole Using a Three-Dimensional Search Technique. *J. Med. Chem.* **1995**, *38*, 2728−2741.
(12) Marriott, D. P.; Dougall, I. G.; Meghani, P.; Liu, Y.; Flower, D. R. Lead Generation Using Pharmacaophore Mapping and 3D Database Searching: Application to Muscarinic M3 Receptor. *J. Med. Chem.* **1999**, *42*, 3210−3216.
(13) *Available Chemical Directory*; MDL: San Leandro, CA, 1998.
(14) Jones, E. Y.; Harlos, K.; Bottomley, M. J.; Robinson, R. C.; Driscoll, P. C.; Edwards, R. M.; Clements, J. M.; Dudgeon, T. J.; Stuart, D. I. Crystal structure of an integrin-binding fragment of vascular cell adhesion molecule-1 at 1.8 Å resolution. *Nature* **1995**, *373*, 539−544.
(15) Lobb, R. R.; Antognetti, G.; Pepinsky, R. B.; Burkly, L. C.; Leone, D. R. et al. A Direct binding assay for the vascular cell adhesion molecule-1 (VCAM-1) interaction with alpha4 integrins. *Cell Adhes. Commun.* **1995**, *3*, 385−397.

JM020054E